

Thin Film Refractive Index and Thickness

Paulo Lourenço^{1b,c}, Manuela Vieira^{a,b,c}, Alessandro Fantoni^{a,c}

^a ISEL - Instituto Superior de Engenharia de Lisboa, Instituto Politécnico de Lisboa
Rua Conselheiro Emídio Navarro, 1, 1959-007 Lisboa, Portugal;

^b Faculdade de Ciências e Tecnologia, FCT, Universidade Nova de Lisboa
Departamento de Engenharia Eletrotécnica, Campus da Caparica, 2829-516 Caparica,
Portugal;

^c CTS-UNINOVA, Campus da Caparica, 2829-516 Caparica, Portugal

Abstract. Integrated optics are a contemporaneous reality in which thin-film technology and methods utilized in the development of integrated circuitry, are applied to both optical circuits and devices. This provides systems that show improved characteristics when compared to their electronic counterparts. Optical systems enable wider bandwidth operation, less power consumption, more immunity to interference and higher cost-efficiency. These features definitely represent a huge improvement in our daily lives when completely embedded in Information and Communications Technologies, replacing a large percentage of contemporaneous electronic based systems. The building blocks of these optical systems consist on waveguides and structures formed by deposited thin films. Two characteristics of utmost importance for these structures are the height and refractive index of the deposited film. In this work and by using a prism coupler, we will be presenting an optical setup and the experimental method that is used to determine both refractive index and thickness of the wave guiding structure.

Keywords: thin film, refractive index and thickness determination method, optical setup, prism coupling.

1 Introduction

Electromagnetic (EM) radiation is present anywhere and propagates through open space linearly spreading its initial beam's cross section, when unperturbed by any other physical phenomenon or obstacle. Nevertheless, EM energy may be confined within a structure and guided propagation may take place if proper circumstances are given. Confinement and propagation of EM radiation within a structure is governed by a phenomenon known as Total Internal Reflection (TIR), which consists on consecutive reflections of the EM wave on the structure's internal boundaries.

Contemporaneous need for integrated photonics is a reality. Laser beams can be guided into thin film structures, where manipulating processes such as modulation, switching, frequency conversion and more, may be accomplished entirely within these

¹ pj.lourenco@campus.fct.unl.pt

structures. Assembling all components of a system within the same structure will contribute to the reduction of ambient conditions effects, an increase of reliability, lower systems' footprint and increase their cost-effectiveness. Moreover, the thickness of these structures is in the order of hundreds of nanometres. This enables the propagation of EM waves with very high power densities by unit area, which is beneficial for both electro-optic conversion and non-linear effects. These features may then be exploited to further promote photonics integration.

Photonic Integrated Circuits (PIC) are assembled through the deposition of consecutive material layers. These are thin layers, few hundreds of nanometres thick, of a given material and their optical properties are different from bulk material properties. In order to fabricate these photonic systems, one must know the optical properties of each deposited layer. This brings us to this paper main driving research purpose:

- Is it possible to devise an optical setup based on an off-the-shelf laser diode, which is able to determine the optical properties of a given material thin layer?

This document describes the work developed to experimentally quantify, in a non-intrusive way, the refractive index and thickness of deposited thin films. Towards that end, an optical setup has been designed and assembled. The obtained results were verified against simulations executed in a software package [1] implementing the Finite Differences Time Domain (FDTD) numerical method.

The remaining of this paper is organized as follows:

- Next section presents how this document relates to the context of Technological Innovation for Life Improvement, which is the main focus of DoCEIS2020 Doctoral Conference;
- Then follows the Experimental Setup section, where the developed optical setup is presented and correspondent obtained results were post-processed by a developed Matlab application, to provide the refractive index and thickness of the material under analysis;
- Next, it follows the Simulations section, where an FDTD simulation is carried out, considering previously obtained thin film refractive index and thickness to design the workspace. This way, we were able to verify the results obtained both experimental and numerically;
- Finally, there is the Conclusions section where obtained results are gathered, analysed and conclusions are drawn, and reported. Here, future areas of related research will also be discussed.

2 Technological Innovation for Life Improvement Association

Information and Communications Technology (ICT) systems have had an increasing and remarkable relevance in our daily lives for the past few decades and in many sectors of contemporaneous society. Even in traditional sectors of our economy, namely the agricultural sector, technological proliferation is now evident and the overall trend points at an increasing dissemination throughout every aspect of our lives.

Together with this technological proliferation, there has been tremendous achievements focused on the individual's wellbeing and life improvement, and

associated to innovative changes resulting from technology related research. In many ICT research fields, namely optoelectronics/electronics, telecommunications and software development, the specifications for a digital world demand a paradigm change. This will be a fertile ground provider for innovation, with newly developed tools and concepts, and aiming at providing a better and sustainable future, with high quality of life for all mankind.

There has been a number of initiatives concerning the evaluation of the impact and effectiveness of technological development on society, namely literature that addresses ICT applications which were designed to help individuals monitor self-health. From dealing with chronic diseases, to prevent unhealthy behaviour or to facilitate doctor-patient communication. Concurrently, considering design constraints regarding easily understandable information, wearable devices comfort issues, user's motivation and interest over time. Examples of such applications are not difficult to find.

On the other hand, the constant growth of senior population worldwide and its incompatibility with contemporaneous available home and community services, is a reality. Moreover, older citizens with health conditions prefer to remain in familiar living surroundings, instead of moving into health institutions, being them private or public. Lattanzio et al. [2] present a set of research initiatives throughout Europe that intend to deal with the increasing demand for e-health care services and smart technologies. This demand has been generated by a growing elder population with chronic diseases and also for those involved in active aging. The adoption of smart wearable devices is illustrated in an article by Uem et al. [3], where smart wearable devices are used to monitor/collect data and to quantify wellbeing, and health-related quality of life associated to Parkinson's disease condition. This article [3], is substantiated by the real life testimonials of three of its co-authors who, in their turn, have extensive experience dealing with smart wearable devices and that have been enduring with this condition for a long time.

Our work is part of a broader project that consists on the development and characterization of a disposable optoelectronic sensor for point of care detection of Acute Kidney Injury (AKI) biomarkers. This sensing device will be implemented by assembling in one monolithic PIC several individual components. Each of these components will be formed by one or more deposited thin film layers of material on a substrate [4], [5]. For development reasons, it is required to know, as precisely as possible, the refractive index and thickness of each individual deposited thin film layer. Hence, the need to develop a non-intrusive method to determine both refractive index and thickness of the deposited layer. With this purpose in mind, an optical setup has been created and the employed light source is an off-the-shelf semiconductor based lasing device (i. e. a laser diode). The articles in the literature considering this subject mentioned the utilization of hardly inexpensive gas lasers, namely the Argon (Ar) and Helium-Neon (He-Ne) lasers [6]–[11], while our approach considers a common laser diode. This implementation is, to the best of our knowledge, a novel approach to determine thin films refractive indices and their thicknesses.

3 Experimental Setup

Our approach considered the top surface of a Corning glass substrate, where a thin layer of a known semiconductor has been deposited and for which its refractive index and thickness are to be determined; for the remaining of this paper, this assembly will be referred to as the *sample*. Next, a laser beam is focused on the face of an adequately chosen prism (Thorlabs ADT-6 - Rutile Coupling Prism), which has been placed over the sample as depicted in Figure 1. If all possible waveguide modes of the thin film are to be excited, the prism refractive index (n_p) must be higher than the refractive indices of the semiconductor film, gap or substrate (n_f , n_g or n_s , respectively).

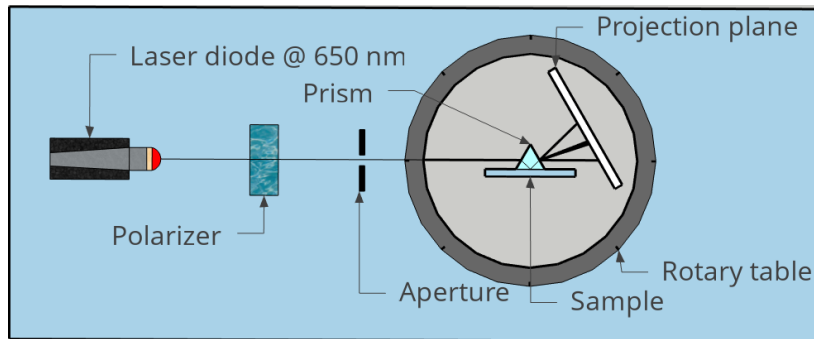


Figure 1 - Optical setup schematic.

On the above figure, one is able to identify the laser diode (Thorlabs L650P007 operating at the 650 nm wavelength) providing the incident plane wave, the polarizer that enables the selection of transversal magnetic (TM) or transversal electric (TE) polarization and an aperture that has been used to minimize the diffraction effects associated to the laser beam. Next follows the rotary table (Thorlabs RBB300A/M), where the sample, prism and projection plane have been securely placed and fastened. This allows their angular motion with the rotary table, while maintaining the prism centred in the rotary table. Prism refractive index is polarization and wavelength dependent, being established through Sellmeier's equations (1) and (2) for TM and TE polarizations, respectively [12]:

$$n^2 = 3.2089 + \frac{3.4000 \times 10^{-5}}{1.2270 \times 10^{-5} - \lambda^{-2}} - 3.2545 \times 10^{-8} \lambda^2 \quad (1)$$

$$n^2 = 2.9713 + \frac{5.1891 \times 10^{-5}}{1.2280 \times 10^{-5} - \lambda^{-2}} - 4.2950 \times 10^{-8} \lambda^2 \quad (2)$$

which, at the 650 nm operating wavelength, yielded the refractive indices 2.5746 and 2.8614 for TM and TE polarizations, respectively.

According to the literature [8], the coupling principles for the excitation of prism-semiconductor film modes may be explained in simple terms:

- Incoming laser beam goes through the prism face and is totally reflected at the base of the prism;
- Total reflection of the laser beam generates a standing wave inside the prism and, consequently, an evanescent field extending from its base into the air gap below;
- Boundary conditions of EM fields at the prism base require that fields below and above the prism base propagate with the same wave motion, thus the evanescent field varies in the z-axis as $e^{(ikn_3z \sin \theta_3)}$;
- If the air gap spacing is thin enough ($< \lambda_0/2$), the evanescent field penetrates into the semiconductor film and may excite a propagating mode (phenomenon described as optical tunnelling);
- If the x-axis component of the wave vector mode in the film, which varies in the z-axis as $e^{(ikn_1z \sin \theta_1)}$, coincides with the correspondent component of the evanescent field below the prism base, the EM wave inside the prism is exclusively coupled to the waveguide mode and the laser beam is considered to be in a synchronous direction;
- Hence, it is possible to couple the EM standing wave developed within the prism to any semiconductor film mode by selecting the correct synchronous direction for the incoming laser beam.

Figure 2 shows in a) the propagation of the EM field within the a-SiNx:H thin film. The streak of light observed reveals some brighter points which might indicate surface roughness on the deposited thin film. Figure 2b) shows the first generated line on the projection plane as the prism is rotated counter-clockwise. Figure 2c) presents the projection plane at a later stage of the prism rotation. The bright light point indicated as “angular position” moves horizontally on the projection plane as “mode line 1” vanishes and “mode line 2” appears. The two marked lines correspond to the fundamental and first modes that are being guided by the a-SiNx:H thin film. The obtained angular synchronous directions, relative to the prism base normal, for the excitation of these modes were:

- 39.8°;
- 48.3°.

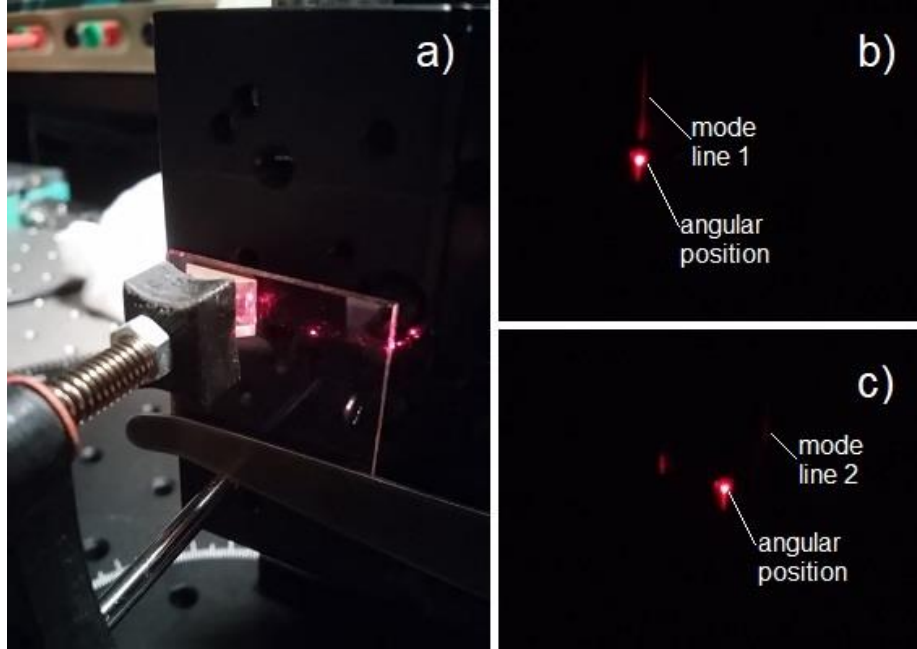


Figure 2 – Experimental results: a) Propagation of light on the thin film; b) Projected line when the fundamental mode is excited on the thin film; c) Projection plane when another mode is excited on the thin film.

According to Tien et al. [6], the incident beam on the prism base must have the right angle of incidence for its associated evanescent field phase velocity matches the phase velocity of the propagating mode in the semiconductor. The component of the propagating vector, parallel to the thin film, inside the prism is $kn_p \sin \theta_p$, where $k = \omega/c$ is the wave number, ω is the angular frequency and c is the speed of light in free space. Considering β_m as the propagation constant of the mode in the wave guiding film, a synchronous direction θ_p of the standing wave generated inside the prism is verified when:

$$\beta_m = k n_p \sin \theta_p \quad (3)$$

After calculating the modal indices of the excited modes, these parameters were fed into a developed Matlab application which returning outcome are the refractive index and thickness of the semiconductor wave guiding structure. The obtained results for this sample were:

$$a = 6.016695e - 01 \mu m, n = 2.365337e + 00,$$

where a and n represent thin film thickness and refractive index, respectively.

4 Simulations

The experimental setup provided the angle readings for the encountered synchronous directions. This data has been processed by a developed Matlab routine which computed the refractive index and thickness of our sample. Nevertheless, to confirm the obtained results, a simulation workspace has been designed on a known and well established software [1]. This software includes a package [13] to perform FDTD numerical method simulations and which has been utilized to conduct the verification of the obtained experimental results.

Simulations considered a plane wave at the operating wavelength of 650 nm, propagating within a dielectric medium, which refractive index matches the rutile prism refractive index that has been used in the experimental setup. This plane wave direction is aimed at the separation interface between this dielectric medium and an air gap, representing the rutile prism base and its separation gap from the sample, respectively. The sample is represented in the simulation by two adjacent media. First, a medium which refractive index and thickness correspond to the outcome obtained by previously executed Matlab computation of experimental data. Then, a second medium that emulates the Corning glass on which the semiconductor film has been deposited.

The working principle of the simulation consisted on iterating the plane wave incidence angle, at the separating interface between the first dielectric medium (rutile prism) and the air gap, while monitoring the correspondent reflection. According to Ulrich et al. [14], a laser beam coupling through a prism into a planar dielectric film is governed by the angle of incidence θ of the beam onto the prism base. This angle corresponds to the phase velocity $v_p = c/n_p \sin \theta$ in the propagation direction of the wave in the prism (refractive index n_p) and in the air gap. Exclusive coupling of EM energy into the semiconductor film occurs only when v_p matches one of the phase velocities of the modes allowed within the film v_m (where $m = 0,1,2, \dots$). Hence, by determining the synchronous angles θ_m that correspond to the strongest coupling, one is able to infer the propagation constant, relatively to the propagation constant of vacuum ($k_0 = \omega_0/c$), of each allowed mode of a given semiconductor film,

$$n_{rel}^m = c/v_m = n_p \sin \theta_m \quad (4)$$

Figure 3 represents the simulation workspace where it is possible to identify, from left to right, the dielectric medium associated to the rutile prism (light blue area), the first thick line representing the reflected energy monitor (dark green area) and the plane wave which incidence angle is to be iterated (orange line). Follows the air gap (white area), the thin semiconductor film (red area), the dielectric medium associated to the Corning glass on which the film has been deposited (blue rectangle) and the second thick line representing the transmission monitor (dark green area). The purple rectangular line sets the simulation domain limits.

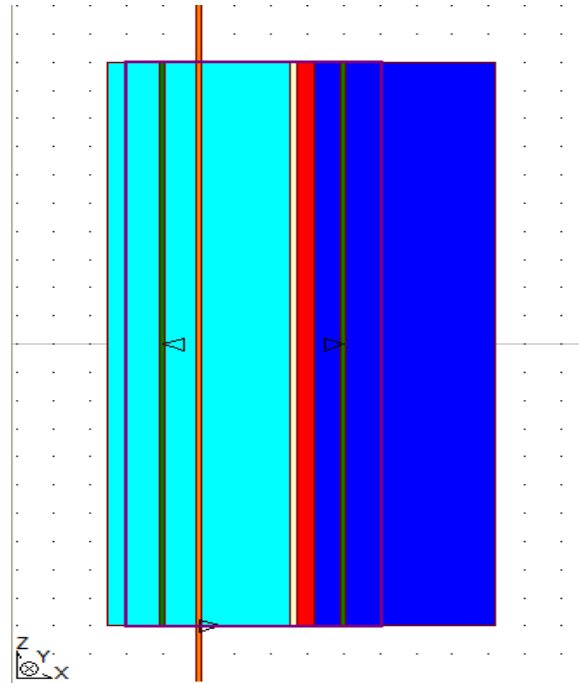


Figure 3 - FDTD simulation workspace.

FDTD simulations have been carried out considering an iterated incidence angle initiating at 30° and ending at 80° , while monitoring the reflected energy amplitude by the separation interface between the dielectric and the air gap. Boundary conditions were set to Perfectly Matched Layer (PML) and grid and step sizes were set to obtain convergence of the FDTD algorithm and realistic results. The air gap width has been set to 100 nm for it should be within a quarter to an eighth of the operating wavelength [8].

Results obtained in simulations for monitored reflected beam power show three dips as presented in Figure 4. These three features correspond to the three allowed modes, considering the operating wavelength and the thin film characteristics. These modes have been excited within the semiconductor film while the plane wave incidence angle has been iterated and correspond to the synchronous directions of 47.5° , 51.5° and 55° .

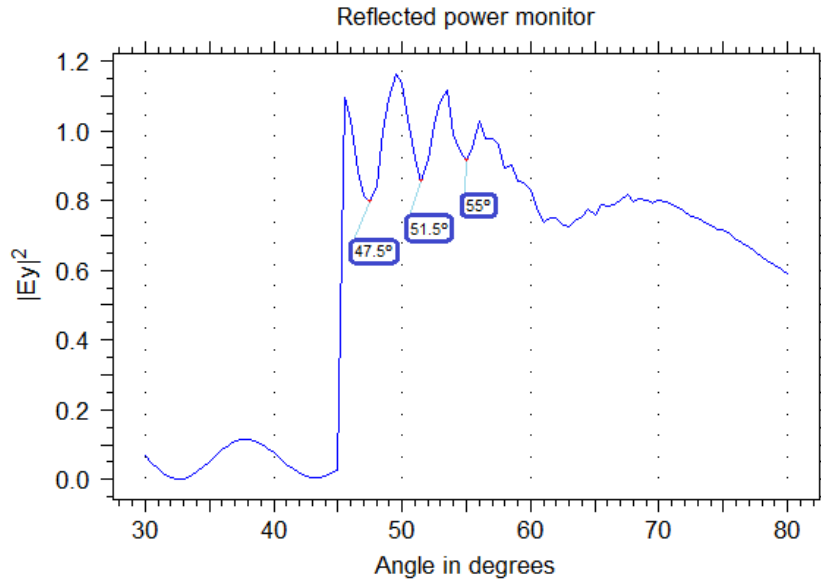


Figure 4 - Synchronous directions obtained in simulations.

Considering that, the presented synchronous directions in Figure 4 have as zero angle reference the x-axis and that the positive angle direction is anti-clockwise, the angles obtained experimentally (39.8° and 48.3°) are their $\pi/2$ complement for they are measured against the normal at the plane of incidence. Also, the experimental synchronous directions were visually acquired and annotated, which is definitely prone to errors. Plus, thin film surface roughness plays a decisive role when it comes to efficient coupling of the evanescent field, at the base of the prism, into the thin film waveguide. Moreover, both simulations and experimental readings revealed a range of several degrees that are able to excite the mode under observation, instead of being a selective and precise direction.

5 Conclusions

The refractive index and thickness determination of a semiconductor thin film has been accomplished experimentally through the development and implementation of an optical setup and the prism coupling method. The synchronous directions obtained by observing the prism projected reflections on a screen were, subsequently, used as input parameters of a developed Matlab implementation. The outcome result of the processing software were the thin film sample refractive index and thickness. To confirm these results, an FDTD simulation workspace has been developed and executed, considering previously obtained sample refractive index and thickness.

Some discrepancies were noted between the results obtained experimentally and the ones acquired through simulation, but it may be explained by the lack of precision of experimental visual readings, by an excessive surface roughness and by existing a range of synchronous directions which are able to excite a particular mode.

Future work will consist on the evaluation of different samples, improvement of synchronous directions experimental readout, verification/improvement of Matlab application and attempt to verify/quantify the correlation between thin film surface roughness and the verified results' discrepancies.

Acknowledgements: This research has been supported by EU funds through the FEDER European Regional Development Fund and by Portuguese national funds provided by FCT – Fundação para a Ciência e a Tecnologia through grant SFRH/BD/144833/2019 and projects PTDC/NAN-OPT/31311/2017 and UID/EEA/00066/2019, and by projects IPL/2019/BioPlas_ISEL and IPL/2019/MO-TFT_ISEL.

References

1. "Synopsys RSoft Solutions." [Online]. Available: <https://www.synopsys.com/optical-solutions/rsoft.html>. [Accessed: 02-Nov-2019].
2. F. Lattanzio *et al.*, "Advanced technology care innovation for older people in Italy: Necessity and opportunity to promote health and wellbeing," *J. Am. Med. Dir. Assoc.*, vol. 15, no. 7, pp. 457–466, 2014.
3. J. M. T. Van Uem *et al.*, "A viewpoint on wearable technology-enabled measurement of wellbeing and health-related quality of life in Parkinson's disease," *J. Parkinsons. Dis.*, vol. 6, no. 2, pp. 279–287, 2016.
4. P. Lourenço, A. Fantoni, J. Costa, and M. Vieira, "Lithographic mask defects analysis on an MMI 3 dB splitter," *Photonics*, vol. 6, no. 4, pp. 1–8, 2019.
5. A. Fantoni, J. Costa, M. Fernandes, Y. Vygranenko, and M. Vieira, "A simulation analysis for dimensioning of an amorphous silicon planar waveguide structure suitable to be used as a surface plasmon resonance biosensor," in *Fourth International Conference on Applications of Optics and Photonics*, 2019, p. 28.
6. P. K. Tien, R. Ulrich, and R. J. Martin, "Modes of propagating light waves in thin deposited semiconductor films," *Appl. Phys. Lett.*, vol. 14, no. 9, pp. 291–294, 1969.
7. P. K. Tien and R. Ulrich, "Theory of Prism–Film Coupler and Thin-Film Light Guides," *J. Opt. Soc. Am.*, vol. 60, no. 10, pp. 1325–1337, 1970.
8. P. K. Tien, "Light Waves in Thin Films and Integrated Optics," *Appl. Opt.*, vol. 10, no. 11, pp. 2395–2413, 1971.
9. P. K. Tien, G. Smolinsky, and R. J. Martin, "Thin Organosilicon Films for Integrated Optics," *Appl. Opt.*, vol. 11, no. 3, pp. 637–642, Mar. 1972.
10. R. T. Kersten, "A new method for measuring refractive index and thickness of liquid and deposited solid thin films," *Opt. Commun.*, vol. 13, no. 3, pp. 327–329, 1975.
11. A. C. Adams, D. P. Schinke, and C. D. Capio, "An Evaluation of the Prism Coupler for Measuring the Thickness and Refractive Index of Dielectric Films on Silicon Substrates," *J. Electrochem. Soc.*, vol. 126, no. 9, pp. 1539–1543, 1979.
12. "Coupling prisms - Thorlabs." [Online]. Available: https://www.thorlabs.com/newgrouppage9.cfm?objectgroup_id=3243. [Accessed: 28-Dec-2019].

13. "FullWAVE - FDTD method." [Online]. Available: <https://www.synopsys.com/photonic-solutions/rsoft-photonic-device-tools/passive-device-fullwave.html>. [Accessed: 29-Dec-2019].
14. R. Ulrich and R. Torge, "Measurement of Thin Film Parameters with a Prism Coupler," *Appl. Opt.*, vol. 12, no. 12, p. 2901, 1973.